Characterization of Asymmetric Coupled CMOS Lines

Uwe Arz[1], Dylan F. Williams[2], David K. Walker[2], Janet E. Rogers[2],
Markus Rudack[1], Dieter Treytnar[1], Hartmut Grabinski[1]

[1] Laboratorium für Informationstechnologie, Universität Hannover
Schneiderberg 32, 30167 Hannover, Germany
Ph: [+49] 511.762.5056 Fax: [+49] 511.762.5051 E-mail: uwe@lfi.uni-hannover.de

[2] National Institute of Standards and Technology, 325 Broadway, Boulder, CO 80303

***Abstract*- This paper investigates the properties of asymmetric coupled lines built in a 0.25 µm CMOS technology in the frequency range of 50 MHz to 26.5 GHz. We show that the frequency-dependent line parameters extracted from calibrated four-port S-parameter measurements agree well with data predicted by numerical calculations. To our knowledge these are the first complete high-frequency measurements of the line parameters for asymmetric coupled lines on silicon ever reported.**

INTRODUCTION

We studied the coupled lines shown in Fig. 1. These lines were fabricated in a six-level-metal process. We will refer to the lowest level of metal as metal 1 (M1 in the figure) and the top level of metal as metal 6 (M6 in the figure). The two coupled conductors are fabricated in metal 2, and have widths of 1 µm and 10 µm, and are separated by a gap of 1 µm. The thickness of metal 2 is 0.7 µm, and its conductivity is 27.8 x 10 ^{6} S/m. The asymmetric coupled lines are surrounded by 20 µm wide grounds that are connected to the substrate with via arrays connected through all six metallization layers.

Fig. 2 shows the top view of the coupled-line test structures. We used on-wafer probes to connect to four 50 µm by 50 µm contact pads fabricated in the top metal layer (metal 6). These are labeled ports 1-4 in Fig. 2. Vias from metal 6 to metal 2 connect the signal pads to the access lines of the coupled line system in metal 2. The width of the access lines is 1 µm, and their length is 200 µm. We fabricated these coupled lines with lengths of 0.5 mm, 1.0 mm and 2.5 mm.

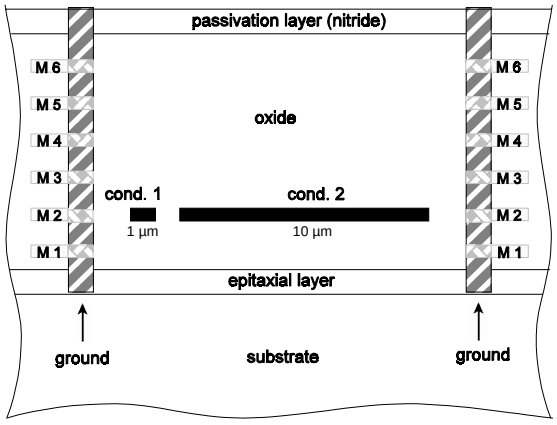

Fig. 1. Cross section of the coupled lines.

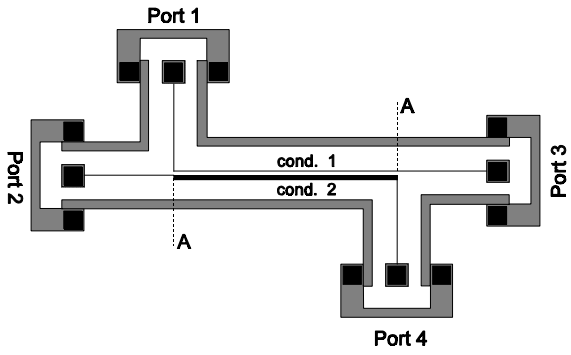

Fig. 2. Top view of the test structures.

The test structures differ from the experimental setup described in [1] in several important aspects. The skin effect in the conductive substrate leads to an even more complex frequency-dependent behavior. Vias connecting the contact pads, which are fabricated in metal 6, and the signal lines, which are fabricated in metal 2, have to be taken into account. In addition, the access lines in metal 2 that connect the contact pads and the coupled line segment are subject to the same substrate effects as the coupled line segment, and must also be accounted for. There are also small electrical discontinuities where the 1 μm wide access lines connect to the coupled-line segment, which we ignored in the analysis.

MEASUREMENT PROCEDURE

We used two-port measurements to characterize the contacts and access lines. We first performed a 50 Ω multiline thru-reflect-line (TRL) reference calibration [2] in coplanar lines fabricated on a semi-insulating gallium arsenide substrate, and moved the calibration reference plane back to the probe tips. We then performed a second-tier TRL calibration to a reference plane in the access lines fabricated on the silicon substrate. The reference impedance of this calibration was equal to the characteristic impedance of the access lines.

Here we employed the "calibration comparison" method [3], which is insensitive to large contact-pad capacitance, to determine the characteristic impedance of the access lines. We then used this information to reset the reference impedance of the second-tier calibration to 50 Ω. This procedure determined an "error box" describing the electrical parameters of the contact pads, vias and access lines.

The calibration procedure used for the four-port measurement is described in [4]. It eliminates the need for orthogonal calibration standards and requires only three in-line calibrations. To this end, we used the multiline TRL procedure [2] and our coplanar standards to perform a 4-port probe-tip calibration.

Since the initial reference plane position of the four-port calibration was "at the probe tips", we used the error boxes we determined earlier to move the reference planes to the position labeled A at the beginning of the coupled-line segment in Fig. 2.

LINE PARAMETERS

The coupled lines support two dominant modes, which are commonly called the c and π modes, and which correspond to the even and odd modes in the symmetric case. The relationship between modal (subscript m) and conductor representations (subscript c) of voltage and current vectors in a multiconductor transmission line is given by $\boldsymbol{v}_c = \boldsymbol{M}_v \boldsymbol{v}_m$ and $\boldsymbol{i}_c = \boldsymbol{M}_i \boldsymbol{i}_m$, where the transformation matrices $\boldsymbol{M}_v$ and $\boldsymbol{M}_i$ are defined in [5]. The vectors $\boldsymbol{v}_c$ and $\boldsymbol{i}_c$ are power-normalized. These vectors satisfy the transmission line equations $d\boldsymbol{v}_c/dz = -\boldsymbol{Z}_c \boldsymbol{i}_c$ and $d\boldsymbol{i}_c/dz = -\boldsymbol{Y}_c \boldsymbol{v}_c$, where the matrices of conductor impedances and admittances per unit length are defined by $\boldsymbol{Z}_c \equiv \boldsymbol{R}_c + j\omega \boldsymbol{L}_c$ and $\boldsymbol{Y}_c \equiv \boldsymbol{G}_c + j\omega \boldsymbol{C}_c$.

We determined the matrices of the line parameters $\boldsymbol{R}_c$, $\boldsymbol{L}_c$, $\boldsymbol{G}_c$, and $\boldsymbol{C}_c$, in the conductor representation of [5]. The voltage paths were chosen between each of the two conductors and the ground. In our analysis we ignored the four-port error boxes representing the discontinuities between the single-mode access lines and the multi-mode coupled-line segment, which we believed to be small.

We estimated $\boldsymbol{R}_c$, $\boldsymbol{L}_c$, $\boldsymbol{G}_c$, and $\boldsymbol{C}_c$ from the four-port measurement data using the weighted orthogonal distance regression algorithm of [6], and the procedure described in [1]. This procedure solved for the elements of $\boldsymbol{R}_c$, $\boldsymbol{L}_c$, $\boldsymbol{G}_c$, and $\boldsymbol{C}_c$ at each frequency point independently. We calculated the starting values for the lowest frequency point with the method of [7], and then used the optimization results at each frequency point as starting values for the optimization at the next higher frequency point.

The estimation procedure of [6] also gives 95% confidence intervals for the estimated results based on the assumption that the error sources in the

experiment are entirely random, independent, and normally distributed.

Figures 3, 4, and 5 show the measured and calculated line parameters of the asymmetric coupled line system, and the 95% confidence intervals. The calculations were performed with the quasi-analytical formulas of [7]. The values of $\boldsymbol{G}_c$, which are not presented here, are all smaller than 0.02 S/cm over the whole frequency range, and do not have a significant effect on the signal propagation behavior of the coupled line system.

CONCLUSION

The agreement between measured and calculated values is good over the entire frequency band. However, some of the calculated values fall outside of the 95% confidence intervals for the estimated parameters. This is a clear indication that there is still some systematic error in either the measurements or calculations. Possible sources of systematic error in the measurements include our neglect of the four-port error boxes that describe the transition between the access lines and coupled-line segments. Errors in the calculations can probably be traced back to uncertainties in the information supplied by the manufacturer on the cross-sectional parameters of the six-metal-layer CMOS process.

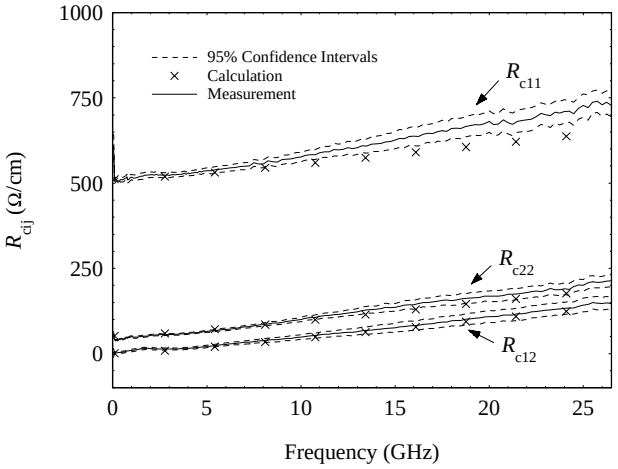

Fig. 3. Resistance per unit length of the coupled lines.

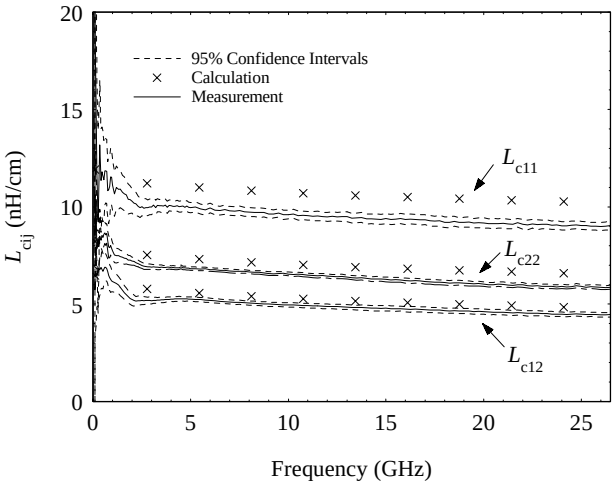

Fig. 4. Inductances per unit length of the coupled lines.

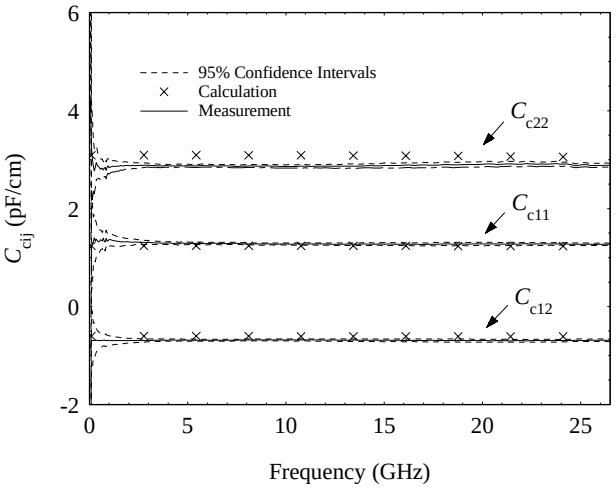

Fig. 5. Capacitances per unit length of the coupled lines. C_{c12} is negative due to the definitions used to define the conductor current (see Fig. 4 of [5]).

REFERENCES

[1] D. F. Williams, J. E. Rogers, and C. L. Holloway, "Multiconductor Transmission Line Characterization: Representations, Approximations, and Accuracy", *IEEE Trans. Microwave Theory and Tech.*, vol. 47, no. 4, pp. 403-409, April 1999.

[2] R. B. Marks, "A Multiline Method of Network Analyzer Calibration", *IEEE Trans. Microwave Theory and Tech.*, vol. MTT-39, no. 7, pp. 1205-1215, July 1991.

[3] D. F. Williams, U. Arz, and H. Grabinski, "Accurate Characteristic Impedance Measurement on Silicon", *1998 IEEE MTT-S Symposium Dig.*, pp. 1917-1920, June 9-11, 1998.

[4] D. F. Williams and D. K. Walker, "In-line Multiport Calibration", *51st ARFTG Conf. Dig.*, pp. 88-90, June 12, 1998.

[5] D. F. Williams, L. A. Hayden, and R. B. Marks, "A Complete Multimode Equivalent-Circuit Theory for Electrical Design", *J. Res. Natl. Inst. Stand. Technol.*, vol. 102, no. 4, pp. 405-423, July -Aug. 1997.

[6] P. T. Boggs, R. H. Byrd, and R. D. Schnabel, "A Stable and Efficient Algorithm for Nonlinear Orthogonal Distance Regression", *SIAM J. Sci. Stat. Comput.*, pp. 1052-1078, Nov. 1987.

[7] E. Grotelüschen, L. S. Dutta and S. Zaage, "Quasi-analytical Analysis of the Broadband Properties of Multiconductor Transmission Lines on Semiconducting Substrates", *IEEE Trans. Comp., Packag., and Manufact. Tech.-Part B*, vol. 17, pp. 376-382, Aug. 1994.